Cardiac Na^+ Channel Dysfunction in Brugada Syndrome Is Aggravated by β_1-Subunit

Naomasa Makita, MD, PhD; Nobumasa Shirai, MD; Dao W. Wang, MD; Koji Sasaki, MD; Alfred L. George, Jr, MD; Morio Kanno, MD, PhD; Akira Kitabatake, MD, PhD

Background—Mutations in the gene encoding the human cardiac Na^+ channel α-subunit (hH1) are responsible for chromosome 3–linked congenital long-QT syndrome (LQT3) and idiopathic ventricular fibrillation (IVF). An auxiliary β_1-subunit, widely expressed in excitable tissues, shifts the voltage dependence of steady-state inactivation toward more negative potentials and restores normal gating kinetics of brain and skeletal muscle Na^+ channels expressed in *Xenopus* oocytes but has little if any functional effect on the cardiac isoform. Here, we characterize the altered effects of a human β_1-subunit (hβ_1) on the heterologously expressed hH1 mutation (T1620M) previously associated with IVF.

Methods and Results—When expressed alone in *Xenopus* oocytes, T1620M exhibited no persistent currents, in contrast to the LQT3 mutant channels, but the midpoint of steady-state inactivation ($V_{1/2}$) was significantly shifted toward more positive potentials than for wild-type hH1. Coexpression of hβ_1 did not significantly alter current decay or recovery from inactivation of wild-type hH1; however, it further shifted the $V_{1/2}$ and accelerated the recovery from inactivation of T1620M. Oocyte macropatch analysis revealed that the activation kinetics of T1620M were normal.

Conclusions—It is suggested that coexpression of hβ_1 exposes a more severe functional defect that results in a greater overlap in the relationship between channel inactivation and activation (window current) in T1620M, which is proposed to be a potential pathophysiological mechanism of IVF in vivo. One possible explanation for our finding is an altered α-/β_1-subunit association in the mutant. **(*Circulation*. 2000;101:54-60.)**

Key Words: action potentials ■ arrhythmia ■ death, sudden ■ electrophysiology ■ fibrillation

Idiopathic ventricular fibrillation (IVF) is a clinical disorder characterized by development of ventricular fibrillation without obvious structural heart disease. It is believed to account for 3% of survivors of out-of-hospital cardiac arrest.[1] In 1992, Brugada and Brugada[2] described 8 patients with unique ECG findings consisting of right bundle-branch block and ST-segment elevation in leads V_1 through V_3, normal Q-T interval, and aborted cardiac death. This is now called the Brugada syndrome and represents a distinct syndrome of IVF. The clinical features of the Brugada syndrome can be attributed to early repolarization, depolarized areas of right ventricular myocardium, or focal right ventricular conduction abnormalities.[3]

Recent genetic studies have confirmed that the Brugada syndrome and chromosome 3–linked congenital long-QT syndrome (LQT3) are allelic disorders of the cardiac Na^+ channel α-subunit gene (*SCN5A*, 3p21).[4,5] At present, 3 *SCN5A* mutations have been demonstrated in the Brugada syndrome: a splice-donor mutation, a frame-shift mutation, and a missense mutation.[5] The missense mutation, T1620M, results in substitution of methionine for Thr1620 located at the extracellular linker between segments S3 and S4 of domain 4 (D4/S3-S4) of the human cardiac Na^+ channel α-subunit (hH1)[6] (Figure 1). T1620M mutant channels expressed in *Xenopus* oocytes showed a shift of voltage dependence of steady-state inactivation toward more positive potentials and 20% to 30% acceleration of recovery from inactivation.[5] Persistent currents due to channel reopening, a molecular basis for QT prolongation in LQT3,[7–9] were not evident in T1620M.[5] It is not clear, however, whether these rather subtle functional defects of T1620M are sufficient to cause ECG abnormalities and predisposition to lethal ventricular arrhythmias in Brugada syndrome patients or whether some other factors involved in the functional association with mutant channel molecules may give rise to aggravation of the biophysical abnormality in vivo.

Voltage-gated Na^+ channels are heteromultimeric complexes of a large, heavily glycosylated α-subunit and 1 or 2 smaller β-subunits.[10] For heterologous expression of recombinant Na^+ channels in *Xenopus* oocytes, an α-subunit alone is usually sufficient to form functional channels, whereas β-subunits may be required for normal gating.[11] The β_1-

Received May 20, 1999; revision received July 21, 1999; accepted August 4, 1999.

From the Department of Cardiovascular Medicine (N.M., N.S., K.S., A.K.) and Department of Pharmacology (M.K.), Hokkaido University School of Medicine, Sapporo, Japan, and the Departments of Medicine and Pharmacology, Vanderbilt University School of Medicine (D.W.W., A.L.G.), Nashville, Tenn.

Correspondence to Naomasa Makita, MD, PhD, Department of Cardiovascular Medicine, Hokkaido University School of Medicine, Kita-15, Nishi-7, Kita-Ku, Sapporo 060-8638, Japan. E-mail makitan@med.hokudai.ac.jp

Circulation **is available at http://www.circulationaha.org**

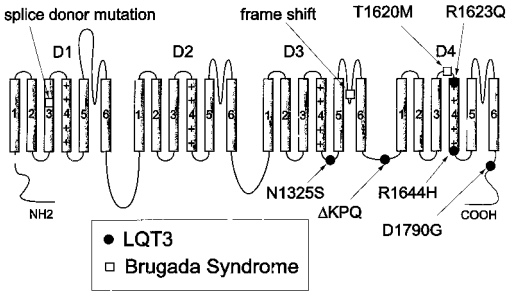

Figure 1. Predicted membrane topology of human cardiac Na^+ channel α-subunit (hH1) and location of Brugada syndrome (□) and LQT3 mutations (●). Four hydrophobic domains (D1-D4), each consisting of 6 transmembrane α-helices (S1-S6), are linked by interdomains. Interdomain connecting D3 and D4 is believed to be the essential structure for fast inactivation, and positively charged α-helix (S4) in each domain is believed to be the essential structure for voltage sensor. Missense mutation T1620M is located at extracellular linker connecting S3 and S4 of D4. Biochemical consequences of slice donor insertion mutation in intron 7 are not known[5]; however, mutation presumably results in truncation at D1/S3.

subunit greatly accelerates the inactivation of brain and skeletal muscle Na^+ channels expressed in *Xenopus* oocytes. The β_1-subunit also shifts the voltage dependence of steady-state inactivation toward more negative potentials and accelerates recovery from inactivation. It is plausible to infer that the β_1-subunit may modify the functions of T1620M mutant channels if the mutation is located within or adjacent to the structures required for α-/β_1-subunit association.

In this study, we characterize the functional roles of the auxiliary β_1-subunit underlying the pathogenesis of the Brugada syndrome. The heterologously expressed T1620M channel did not show persistent current, in contrast to LQT3 mutant channels; however, it exhibited a shift of voltage dependence of steady-state inactivation toward more positive potentials. Coexpression of a human β_1-subunit (hβ_1) further shifted the midpoint of steady-state inactivation ($V_{1/2}$) and substantially accelerated recovery from inactivation, possibly by destabilizing the inactivation state. Because the activation kinetics of T1620M were near normal, coexpressed hβ_1 exposed a more severe functional defect that resulted in a greater overlap in the relationship between channel inactivation and activation (window current) in T1620M. Because the β_1-subunit is expressed in the heart,[12–14] we propose that these biophysical mechanisms ascribed to aberrant association between α-/β_1-subunits underlie the pathogenesis of the Brugada syndrome.

Methods

Construction of T1620M Mutant Channel cDNA

Amino acid substitution of methionine for Thr1620 (T1620M) of hH1 was performed by an overlap extension polymerase chain reaction (PCR) strategy with 4 oligonucleotide primers: hH1-4418F (5′-TCAACCAACAGAAAAAGT-3′), T1620M-R (5′-GGAAGAGCATCGGGGAGAAGAA-3′), T1620M-F (5′-CTCCCCGATGCTCTTCCGAGT-3′), and hH1-5006R (5′-GCCAAAGATGGAGTAGATGA-3′), as previously described.[9] A 608-bp PCR product was digested with *Bst*EII/*Bam*HI and subcloned back into wild-type hH1 (WT) to assemble the T1620M-hH1 construct. Multiple independent clones were isolated, and their sequence was verified by dideoxynucleotide sequencing of the final constructs.

Heterologous Expression and Electrophysiology

The cDNAs encoding WT, T1620M-hH1 (T1620M), and hβ_1[13] were transcribed in vitro from pSP64T constructs by use of SP6 RNA polymerase, and the resultant sense cRNAs were microinjected into *Xenopus* oocytes and then incubated at room temperature in ND-96 solution (96 mmol/L NaCl, 2 mmol/L KCl, 1.8 mmol/L $CaCl_2$, 1 mmol/L $MgCl_2$, 5 mmol/L HEPES [pH 7.5]) for 1 to 4 days.[13] In some experiments, oocytes were perfused with ND-96 solution with 30 μmol/L tetrodotoxin (TTX; Sigma) to block Na^+ currents and allow determination of TTX-sensitive current component.[8] Whole-cell currents were recorded from oocytes with the 2-microelectrode voltage clamp, as previously described.[13]

Cell-attached macropatch recordings were performed in oocytes with a patch-clamp amplifier (Axopatch 200B, Axon Instruments) based on methods previously described.[15] The patch pipettes had tip resistances of 0.4 to 1.0 MΩ and were filled with ND-96 solution. Recordings were performed with a bath solution predicted to be isopotential and isomolar with the intracellular oocyte milieu and containing 9.6 mmol/L NaCl, 88 mmol/L KCl, 11 mmol/L EGTA, and 5 mmol/L HEPES (pH 7.4). The leak and residual capacitive currents were digitally subtracted online by the P/4 protocol. Patch-clamp recording with cell-attached configuration was used because of its stability, and no significant differences in Na^+ channel kinetics were identified between cell-attached and inside-out configurations. In some experiments, whole-cell patch-clamp recordings were performed with tsA201 cells transfected with either WT or T1620M plasmid in the presence of hβ_1.[7]

To assess steady-state channel inactivation and recovery from inactivation, standard double-pulse protocols were used. Unless otherwise specified, the holding potential was set to −120 mV, and Na^+ currents were recorded during test potentials to −20 mV. For assessment of steady-state inactivation, the membrane potential was stepped to a voltage between −120 and −20 mV for 500 ms, and then peak Na^+ current was measured during a −20 mV test potential. Recovery from inactivation was assessed by a double-pulse protocol consisting of a 500-ms prepulse to 20 mV, which was designed to fully inactivate all channels, followed by a variable-duration interpulse interval (Δt) at various potentials between −80 and −120 mV and a test pulse to −20 mV. The pulse protocol cycle time was 5 seconds unless otherwise stated. Currents were filtered at 5 kHz (−3 dB, 4-pole Bessel filter) and digitized by use of analog-to-digital interface (Digidata 1200, Axon Instruments). Voltage control, data acquisition, and analysis were accomplished by use of pClamp6 software (Axon Instruments). All experiments were performed at 22°C.

Data Analysis

The time course of inactivation was fit with a biexponential function: $I(t)/I_{max}=A_\infty+A_f\times\exp(-t/\tau_f)+A_s\times\exp(-t/\tau_s)$, where A_∞ is a constant value, A_f and A_s are fractions of fast and slow inactivating components, and τ_f and τ_s are the time constants of fast and slow inactivating components, respectively. Conductance curves were computed by use of the equation $G=I/(V_m-E_{rev})$, where G is conductance, I represents the peak test-pulse current, V_m is the test pulse potential, and E_{rev} is the measured reversal potential. Steady-state inactivation and conductance-voltage relationship were fit with the Boltzmann equation $I/I_{max}=\{1+\exp[(V-V_{1/2})/k]\}^{-1}$ to determine the membrane potential for half-maximal activation ($V_{1/2}$) and the slope factor k. We analyzed recovery from inactivation by fitting data using a nonlinear least squares minimization method with a monoexponential equation: $I(t)/I_{max}=A\times\exp(-t/\tau)+C$, where t is the recovery time interval and τ is the time constant of recovery, respectively.

Results were presented as mean±SE. Statistical comparisons were made with the unpaired Student's *t* test to evaluate the significance of the difference between means. Statistical significance was assumed for $P<0.05$.

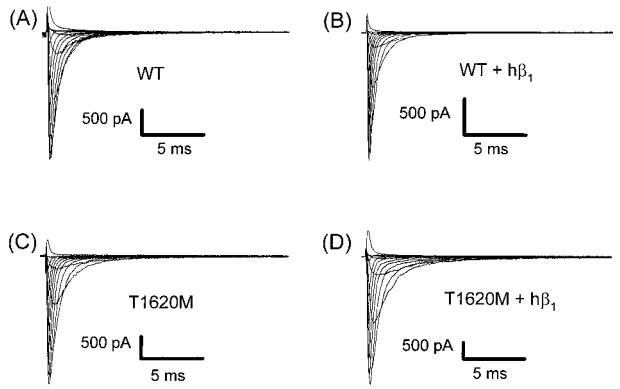

Figure 2. Macroscopic Na^+ currents of WT and Brugada syndrome mutant (T1620M) hH1 channels. A through D, Cell-attached macropatch recordings made in *Xenopus* oocytes expressing WT or T1620M in presence or absence of hβ_1. Currents were elicited by voltage steps in 10-mV increments from −80 to 40 mV. Holding potential was −120 mV.

Results

Onset of Inactivation

Figure 2 shows representative current traces from oocyte macropatches expressing either WT or T1620M in the absence or presence of coexpressed hβ_1. Neither channel allele exhibited persistent currents, the electrophysiological characteristic commonly observed for LQT3 mutations. Furthermore, no detectable TTX-sensitive late Na^+ currents were observed in channels of WT, WT+hβ_1, T1620M, or T1620M+hβ_1 (data not shown). Macroscopic current decays of WT and T1620M in the absence or presence of hβ_1 were fit with a biexponential function. Time constants of the rapidly inactivating component (τ_f) and slowly inactivating component (τ_s) of WT, WT+hβ_1, T1620M, and T1620M+hβ_1 were indistinguishable at all test potentials between −55 and 20 mV (Figure 3A). The fractions of each component were also comparable (data not shown). These data suggest that the onset of inactivation was virtually identical between WT and T1620M and was not affected by the β_1-subunit.

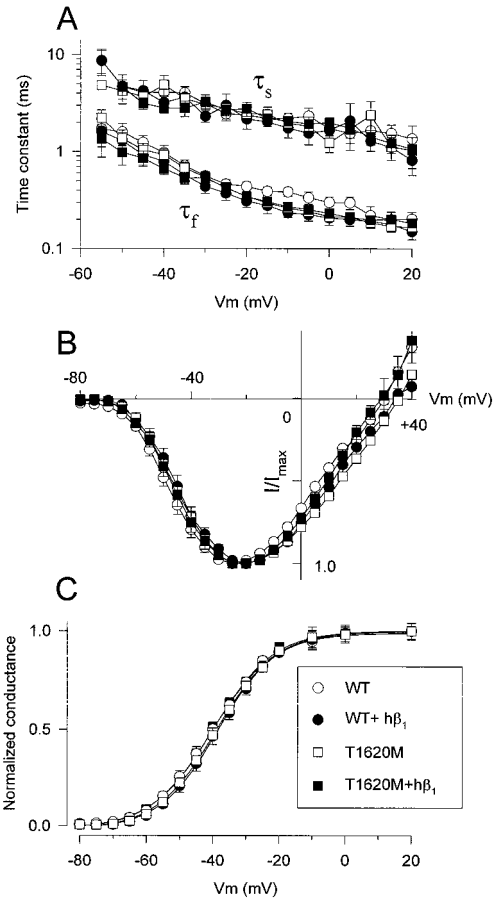

Figure 3. Inactivation and activation properties of WT and T1620M hH1 channel. A, Time constants of current decay of Na^+ current in WT and T1620M expressing oocytes in presence or absence of hβ_1 were measured by macropatch. Current decay at each potential was fit with a biexponential function; time constants of fast (τ_f) and slow (τ_s) components are shown. There were no significant differences in these values among the 4 channels at test potentials between −55 and 20 mV. B, Normalized peak current-voltage relationships. C, Normalized conductance-voltage curves were fit by a Boltzmann relationship. There are no significant differences in $V_{1/2}$ or slope factors among the 4 channels (Table).

Activation, Steady-State Inactivation, and Window Current

Activation kinetics were measured by oocyte cell-attached macropatch techniques. Peak current-voltage relationships (Figure 3B) and peak conductance-voltage relationships (Figure 3C) of WT, WT+hβ_1, T1620M, and T1620M+hβ_1 were nearly superimposable. There were no significant differences in the values of membrane voltage of the midpoint ($V_{1/2}$) and the slope factor (k) for activation among these channels (Figure 3C; Table). These data suggest that the activation kinetics of T1620M were comparable to those of WT, and the β_1-subunit did not alter the activation kinetics of either channel.

Steady-state inactivation was measured by 2-electrode voltage-clamp technique, because this technique usually provides stable recordings and does not exhibit any time-dependent changes in channel inactivation kinetics, which are often observed in patch-clamp recordings.[16] The $V_{1/2}$ and slope factor of steady-state inactivation of WT were −69.2±0.8 mV and 4.2±0.1, respectively, and were not altered by the coexpression of hβ_1 (Figure 4A; Table), consistent with our previous findings.[13] The $V_{1/2}$ of T1620M was significantly (≈5 mV) shifted toward more positive potentials (−64.4±1.0 mV) compared with WT in the absence of hβ_1, with no change in the slope factors (Figure 4B). Coexpression of hβ_1 significantly shifted the $V_{1/2}$ of T1620M further toward more positive potentials (−60.0±0.8 mV, $P<0.001$), whereas the slope factors were not altered. Therefore, coexpression of hβ_1 shifted the voltage dependence of steady-state inactivation of T1620M overall ≈10 mV toward more positive potentials compared with WT without changing the voltage dependence. Because activation kinetics were normal in T1620M and were not affected by the β_1-subunit, coexpression of the β_1-subunit exposed a more severe functional defect that resulted in greater overlap in the relationship between channel inactivation and activation window current in T1620M (Figure 4B). We also observed a similar

Activation and Steady-State Inactivation of WT and T1620M Channels

	WT	WT+hβ_1	T1620M	T1620M+hβ_1
Activation				
$V_{1/2}$, mV	−40.6±1.2	−40.6±1.9	−39.4±1.9	−41.4±0.8
Slope factor, mV	−8.9±0.4	−8.5±0.4	−8.9±0.3	−8.9±0.4
n	9	7	8	9
Inactivation				
$V_{1/2}$, mV	−69.2±0.8	−70.5±0.8	−64.4±1.0*	−60.0±0.8*†
Slope factor, mV	4.2±0.1	4.3±0.1	4.1±0.1	3.8±0.1
n	20	12	21	16

*$P<0.01$ vs WT; †$P<0.001$ vs WT+hβ_1. All activation and inactivation data were obtained by oocyte macropatch and 2-electrode voltage-clamp techniques, respectively.

shift in the voltage dependence of steady-state inactivation for the mutant toward more positive potentials using whole-cell patch clamp of channels expressed in tsA201 cells (WT+hβ_1, $V_{1/2}$= −91.2±0.9 mV, n=7; T1620M+hβ_1, $V_{1/2}$= −87.5±1.2 mV, n=12; $P<0.05$).

Recovery From Inactivation

Recovery from inactivation was assessed by a double-pulse protocol with various recovery potentials by use of the 2-electrode voltage clamp. At a recovery potential of −120 mV, the time courses of recovery from inactivation of WT, WT+hβ_1, and T1620M were nearly superimposable (Figure 5A), consistent with our previous observations that the β_1-subunit does not affect recovery from inactivation of the cardiac α-subunit isoform.[13,17] Recovery from inactivation of T1620M+hβ_1 seemed to be faster than WT+hβ_1 at −120 mV; however, the differences were not statistically significant (Figure 5A). At a recovery potential of −80 mV, hβ_1 remarkably accelerated recovery from inactivation of the T1620M channel (Figure 5B). T1620M without hβ_1 also showed a tendency to recover from inactivation faster than WT or WT+hβ_1; however, no statistically significant differences were observed between them. The time course of recovery from inactivation at each recovery potential was fit with a single-exponential equation, and the time constants were plotted against the recovery potential (Figure 5C). Coexpressed hβ_1 did not alter recovery from inactivation of WT, but it significantly accelerated that of T1620M, and its effects were marked at recovery potentials more positive than −100 mV. Consequently, coexpression of hβ_1 rendered the recovery process of T1620M less voltage dependent. Recovery from inactivation at −80 mV was ≈3 times faster in T1620M+hβ_1 than in WT+hβ_1 (WT+hβ_1, τ=31.9±3.8 ms, n=6; T1620M+hβ_1, τ=10.5±0.9 ms, n=12; $P<0.001$). Increased rate and decreased voltage dependence of recovery from inactivation suggest that the inactivated state of the T1620M mutant channel is destabilized by the β_1-subunit.

Discussion

The present study demonstrates the electrophysiological properties of a cardiac Na^+ channel mutation of the Brugada syndrome (T1620M). The basic properties of the recombinant T1620M mutant channel expressed in *Xenopus* oocytes that were shown in a previous study[5] were (1) a shift of voltage dependence of steady-state inactivation toward more positive potentials and (2) 20% to 30% accelerated recovery from inactivation. Channel dysfunction of T1620M became obvious when oocytes were coinjected with the mutant channel R1232W, which turned out to be a rare polymorphism identified along with T1620M in the affected members of a Brugada syndrome family.[5] However, the biophysical properties of T1620M itself seem to be rather subtle and do not fully explain the severe clinical phenotype or ECG findings of Brugada syndrome patients.[2,18] In the present study, we demonstrate that the Na^+ channel mutation T1620M exhibits not only intrinsic channel dysfunction but also more profound inactivation defects resulting from coexpression of the β_1-subunit. The voltage dependence of steady-state inactivation is further shifted toward more positive potentials (an overall shift of 10 mV compared with WT+β_1; Figure 3), and the recovery from inactivation is markedly accelerated (3 times faster in T1620M+β_1 at a recovery potential of −80 mV compared with WT+β_1; Figure 5). Thus, the β_1-subunit destabilizes the inactivation state of the T1620M mutant channel. Furthermore, because the activation kinetics of T1620M are normal regardless of the presence of the β_1-subunit (Figures 3B and 3C), the positive shift of the steady-state inactivation curve results in greater overlap in the relationships of channel activation and inactivation (Figure 4B). The occurrence of the window current and the destabilized inactivation state will induce hyperexcitability and an arrhythmogenic substrate in Brugada syndrome patients.

Comparison With Congenital LQT Syndrome (LQT3)

The Brugada syndrome and LQT3 are allelic disorders that result from defects in *SCN5A*. The mutated residue Thr1620 of the Brugada syndrome is located at D4/S3-S4, which is in close vicinity to Arg1623, the residue responsible for the de novo LQT3 mutation R1623Q located at the outermost positively charged residue of D4/S4 (Figure 1).[9] Site-directed mutagenesis and functional studies of naturally occurring Na^+ channel mutations have revealed that D4/S3-S4[19] and the neighboring outermost positively charged residue of D4/S4 are implicated in activation-inactivation coupling.[9,20] Despite the adjacency of the residues Thr1620 and Arg1623 of hH1,

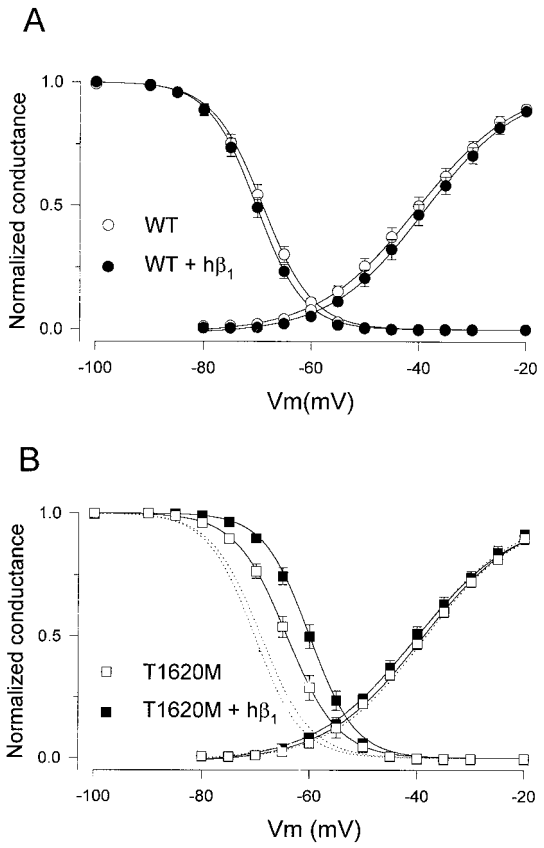

Figure 4. Voltage dependence of steady-state inactivation and activation. A, Steady-state inactivation of WT alone or WT+hβ_1 was measured by oocyte 2-electrode voltage-clamp. Conductance-voltage relationship curves of WT and WT+hβ_1 (Figure 3C) recorded by macropatch are superimposed to show window current. Coexpression of hβ_1 did not alter voltage dependence of steady-state inactivation or conductance-voltage relationships. Consequently, window currents of WT and WT+hβ_1 were comparable (Table). B, Steady-state inactivation of T1620M alone and T1620M+hβ_1. Steady-state inactivation curves and conductance-voltage curves of WT and WT+hβ_1 shown as dotted lines are superimposed as references. $V_{1/2}$ of steady-state inactivation of T1620M was significantly shifted toward more positive potentials, and coexpression of hβ_1 further shifted $V_{1/2}$ in the same direction. Slope factor of inactivation was comparable among 4 channels (Table).

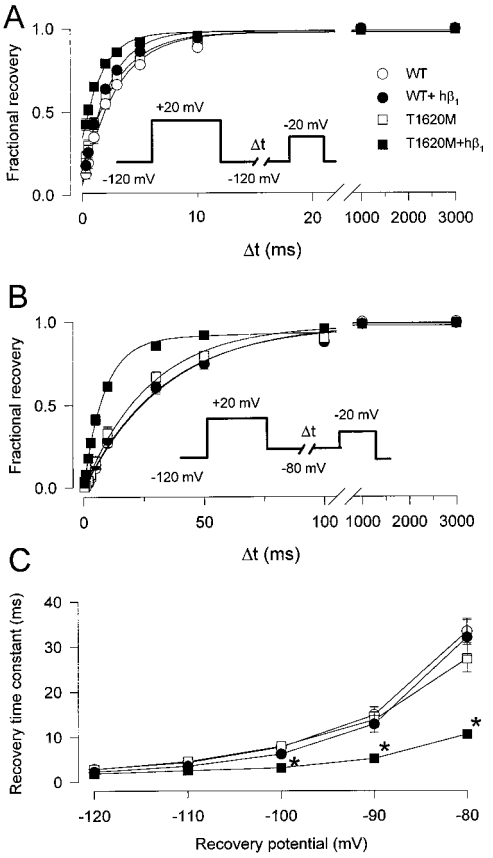

Figure 5. A, Recovery from inactivation at recovery potential −120 mV was recorded from oocyte by 2-electrode voltage-clamp. Time course of recovery of each channel was nearly superimposable and well fit by a single exponential. Recovery time constants were WT, 2.9±0.19 ms (n=11); WT+hβ_1, 2.3±0.15 ms (n=6); T1620M, 2.8±0.17 ms (n=17); and T1620M+hβ_1, 1.7±0.13 ms (n=12). B, Time course of recovery from inactivation at recovery potential −80 mV. Recovery time constants were WT, 33.2±2.4 ms (n=9); WT+hβ_1, 31.9±3.8 ms (n=6); T1620M, 27.2±3.0 ms (n=16); and T1620M+hβ_1, 10.5±1.0 ms (n=12). C, Average time constants vs recovery potential. T1620M showed tendency to recover faster from inactivation at −80 mV; however, it was not significantly different from that of WT or WT+hβ_1. Coexpression of hβ_1 significantly accelerated recovery from inactivation of T1620M at more positive potentials than −100 mV and decreased voltage dependence of recovery process. Recovery time constant of T1620M+hβ_1 was significantly less than those of WT, WT+hβ_1, and T1620M (*$P<0.001$) at recovery potentials between −100 and −80 mV.

the clinical manifestations of the Brugada syndrome (T1620M) and LQT3 (R1623Q) and the biophysical properties of their mutant channels are distinct. The R1623Q patient exhibits a prolonged QT interval on ECG and recurrent episodes of ventricular arrhythmia (torsade de pointes) soon after birth. This malignant clinical phenotype correlates well with the biophysical characteristics. Recombinant R1623Q channels show unusually slow macroscopic inactivation along with persistent Na^+ currents due to prolonged channel opening time and channel bursting behavior.[9] In contrast, T1620M Brugada syndrome patients do not exhibit QT prolongation on ECG. The recombinant T1620M channel does not show late current or slow macroscopic inactivation. These data confirm that the Brugada syndrome and LQT3 are distinct entities from both a clinical and a biophysical standpoint.

Pathophysiological Implications

On the basis of these findings, it is concluded that the β_1-subunit and the mutant α-subunit play significant roles in the pathophysiology of the Brugada syndrome. The β_1-subunit is a small auxiliary protein with a single transmembrane domain. It is widely expressed in excitable cells, such as in brain, nerve, heart, and skeletal muscle, and is encoded by a single gene.[13] It has been demonstrated that the recombinant β_1-subunit modulates the expression levels and gating kinetics of brain[11] and skeletal muscle[13] Na^+ channels in oocytes. When expressed alone, these isoforms exhibit anomalously slow macroscopic inactivation, slow recovery from inactivation, and a positively

shifted steady-state inactivation curve. Coexpression of the β_1-subunit shifts the voltage dependence of steady-state inactivation curves toward more negative potentials and restores normal gating properties of channels observed in native tissues. In contrast to its dramatic effects on brain and skeletal muscle Na^+ channel function, the β_1-subunit has little or no effect on the gating of cloned cardiac Na^+ channels.[13,21]

Structure-function relationships of the α-β_1 interaction have not been elucidated; however, studies with site-directed mutagenesis[22,23] and Na^+ channel–specific toxins[19,24] have provide substantial information. It is believed that α- and β_1-subunits associate in the proximity of the α-scorpion binding sites[25] and that the overlapping region consisting of extracellular portions of D1/S5-S6, D4/S5-S6, and D4/S3-S4 plays an important role in determining the β_1-subunit–induced gating modulation. The mutation T1620M on D4/S3-S4 may alter the physical association between the α- and β_1-subunits of the Na^+ channel, presumably because the residue Thr1620 of the α-subunit could reside within the β_1-subunit binding domain. Alternatively, it is possible that the β_1-subunit interacts elsewhere on the α-subunit, but these structures are coupled allosterically to gating.

Clinical Implications

This study using coexpression of the β_1-subunit clearly demonstrates that the functional abnormalities associated with T1620M are likely to be more severe in vivo than has been shown in oocytes expressing T1620M alone. The expression of both normal and mutated channels in the heart of a patient with Brugada syndrome would promote heterogeneity of the refractory period in myocardium, which in turn serves as an ideal substrate for the development of reentrant arrhythmia.[26] Nevertheless, the functional abnormalities of T1620M identified in the present study do not seem be sufficient to explain all the clinical manifestations observed in the Brugada syndrome. The ECG pattern of the Brugada syndrome has been attributed to the transmural heterogeneity of repolarization of the right ventricular outflow tract. Because the magnitude and duration of the Na^+ current during phase 0 of the cardiac action potential determines the voltage at which phase 1 begins, it is speculated that perturbations in Na^+ currents could have an effect on the kinetics of the transient outward K^+ current (I_{to}), which is predominantly expressed in epicardial cells.[27] Furthermore, the ECG abnormalities of patients with Brugada syndrome transiently normalize during follow-up and subsequently return to the typical pattern,[18] and they are modulated by the autonomic balance and administration of class Ia or Ic antiarrhythmic drugs,[28] which suggests significant roles of the autonomic nervous system in the pathogenesis of the Brugada syndrome. It is not clear whether the mutant channel T1620M (or T1620M+hβ_1) is more susceptible to autonomic nervous system modulations or antiarrhythmic drugs than WT. It is possible that there are additional unidentified Brugada syndrome mutations within *SCN5A*; alternatively, the Brugada syndrome might be a heterogeneous disorder involving multiple responsible genes, as is the case with congenital LQT. The genes encoding I_{to} may be the potential candidates. These hypotheses require further investigation.

Acknowledgments

This work was supported in part by a grant-in-aid for exploratory research, Japan Society of the Promotion of Science (11877008), and the National Institute of Health (NS32387). Dr George is an Established Investigator of the American Heart Association. We thank Drs Christoph Fahlke, Jong-Kook Lee, Noritsugu Tohse, and Masayuki Sakurai for useful discussions.

References

1. Tung RT, Shen WK, Hammill SC, Gersh BJ. Idiopathic ventricular fibrillation in out-of-hospital cardiac arrest survivors. *Pacing Clin Electrophysiol*. 1994;17:1405–1412.
2. Brugada P, Brugada J. Right bundle branch block, persistent ST segment elevation and sudden cardiac death: a distinct clinical and electrocardiographic syndrome: a multicenter report. *J Am Coll Cardiol*. 1992;20:1391–1396.
3. Scheinman MM. Is the Brugada syndrome a distinct clinical entity? *J Cardiovasc Electrophysiol*. 1997;8:332–336.
4. Wang Q, Shen J, Splawski I, Atkinson D, Li Z, Robinson JL, Moss AJ, Towbin JA, Keating MT. SCN5A mutations associated with an inherited cardiac arrhythmia, long QT syndrome. *Cell*. 1995;80:805–811.
5. Chen Q, Kirsch GE, Zhang D, Brugada R, Brugada J, Brugada P, Potenza D, Moya A, Borggrefe M, Breithardt G, Ortiz-Lopez R, Wang Z, Antzelevitch C, O'Brien RE, Schulze-Bahr E, Keating MT, Towbin JA, Wang Q. Genetic basis and molecular mechanism for idiopathic ventricular fibrillation. *Nature*. 1998;392:293–296.
6. Gellens ME, George AL Jr, Chen LQ, Chahine M, Horn R, Barchi RL, Kallen RG. Primary structure and functional expression of the human cardiac tetrodotoxin-insensitive voltage-dependent sodium channel. *Proc Natl Acad Sci U S A*. 1992;89:554–558.
7. Wang DW, Yazawa K, George AL Jr, Bennett PB. Characterization of human cardiac Na^+ channel mutations in the congenital long QT syndrome. *Proc Natl Acad Sci U S A*. 1996;93:13200–13205.
8. Bennett PB, Yazawa K, Makita N, George AL Jr. Molecular mechanism for an inherited cardiac arrhythmia. *Nature*. 1995;376:683–685.
9. Makita N, Shirai N, Nagashima M, Matsuoka R, Yamada Y, Tohse N, Kitabatake A. A de novo missense mutation of human cardiac Na^+ channel exhibiting novel molecular mechanisms of long QT syndrome. *FEBS Lett*. 1998;423:5–9.
10. Catterall WA. Cellular and molecular biology of voltage-gated sodium channels. *Physiol Rev*. 1992;72:S15–S48.
11. Isom LL, De Jongh KS, Patton DE, Reber BF, Offord J, Charbonneau H, Walsh K, Goldin AL, Catterall WA. Primary structure and functional expression of the β1 subunit of the rat brain sodium channel. *Science*. 1992;256:839–842.
12. Sutkowski EM, Catterall WA. β1 Subunits of sodium channels. *J Biol Chem*. 1990;265:12393–12399.
13. Makita N, Bennett PB Jr, George AL Jr. Voltage-gated Na^+ channel β1 subunit mRNA expressed in adult human skeletal muscle, heart, and brain is encoded by a single gene. *J Biol Chem*. 1994;269:7571–7578.
14. Makielski JC, Limberis JT, Chang SY, Fan Z, Kyle JW. Coexpression of β1 with cardiac sodium channel α subunits in oocytes decreases lidocaine block. *Mol Pharmacol*. 1996;49:30–39.
15. Richmond JE, Featherstone DE, Hartmann HA, Ruben PC. Slow inactivation in human cardiac sodium channels. *Biophys J*. 1998;74:2945–2952.
16. Wang DW, George AL Jr, Bennett PB. Comparison of heterologously expressed human cardiac and skeletal muscle sodium channels. *Biophys J*. 1996;70:238–245.
17. Makita N, Bennett PB Jr, George AL Jr. Multiple domains contribute to the distinct inactivation properties of human heart and skeletal muscle Na^+ channels. *Circ Res*. 1996;78:244–252.

18. Brugada J, Brugada P. What to do in patients with no structural heart disease and sudden arrhythmic death? *Am J Cardiol*. 1996;78:69–75.
19. Rogers JC, Qu Y, Tanada TN, Scheuer T, Catterall WA. Molecular determinants of high affinity binding of α-scorpion toxin and sea anemone toxin in the S3–S4 extracellular loop in domain IV of the Na^+ channel α subunit. *J Biol Chem*. 1996;271:15950–15962.
20. Chahine M, George AL Jr, Zhou M, Ji S, Sun W, Barchi RL, Horn R. Sodium channel mutations in paramyotonia congenita uncouple inactivation from activation. *Neuron*. 1994;12:281–294.
21. Qu Y, Isom LL, Westenbroek RE, Rogers JC, Tanada TN, McCormick KA, Scheuer T, Catterall WA. Modulation of cardiac Na^+ channel expression in *Xenopus* oocytes by β1 subunits. *J Biol Chem*. 1995;270:25696–25701.
22. Makita N, Bennett PB, George AL. Molecular determinants of β1 subunit-induced gating modulation in voltage-dependent Na^+ channels. *J Neurosci*. 1996;16:7117–7127.
23. McCormick KA, Isom LL, Ragsdale D, Smith D, Scheuer T, Catterall WA. Molecular determinants of Na^+ channel function in the extracellular domain of the β1 subunit. *J Biol Chem*. 1998;273:3954–3962.
24. Tejedor FJ, Catterall WA. Site of covalent attachment of α-scorpion toxin derivatives in domain I of the sodium channel α subunit. *Proc Natl Acad Sci U S A*. 1988;85:8742–8746.
25. Catterall WA. Structure and function of voltage-sensitive ion channels. *Science*. 1988;242:50–61.
26. Krishnan SC, Antzelevitch C. Sodium channel block produces opposite electrophysiological effects in canine ventricular epicardium and endocardium. *Circ Res*. 1991;69:277–291.
27. Alings M, Wilde A. "Brugada" syndrome: clinical data and suggested pathophysiological mechanism. *Circulation*. 1999;99:666–673.
28. Miyazaki T, Mitamura H, Miyoshi S, Soejima K, Aizawa Y, Ogawa S. Autonomic and antiarrhythmic drug modulation of ST segment elevation in patients with Brugada syndrome. *J Am Coll Cardiol*. 1996;27:1061–1070.

Cardiac Na^+ Channel Dysfunction in Brugada Syndrome Is Aggravated by β_1-Subunit

Naomasa Makita, Nobumasa Shirai, Dao W. Wang, Koji Sasaki, Alfred L. George, Jr, Morio Kanno and Akira Kitabatake

Circulation. 2000;101:54-60
doi: 10.1161/01.CIR.101.1.54
Circulation is published by the American Heart Association, 7272 Greenville Avenue, Dallas, TX 75231

Print ISSN: 0009-7322. Online ISSN: 1524-4539